

## Latest *BABAR* results on radiative penguin B-meson decays and lepton number violation

---

**Fergus WILSON\***<sup>†</sup>

*STFC Rutherford Appleton Laboratory, Chilton, Didcot, Oxon, OX11 0QX, UK*

*E-mail: [Fergus.Wilson@stfc.ac.uk](mailto:Fergus.Wilson@stfc.ac.uk)*

We report on the latest results from *BABAR* for direct  $CP$  asymmetries in  $B \rightarrow X_S \gamma$ , the search for the decays  $B \rightarrow \pi/\eta \ell^+ \ell^-$ , and Lepton Number Violation searches in  $B^+ \rightarrow X^- \ell^+ \ell'^+$  decays

*The European Physical Society Conference on High Energy Physics -EPS-HEP2013  
18-24 July 2013  
Stockholm, Sweden*

---

\*Speaker.

<sup>†</sup>on behalf of the *BABAR* Collaboration

## 1. Direct $CP$ asymmetries in $B \rightarrow X_s \gamma$

The flavor-changing neutral current decay  $b \rightarrow s \gamma$  is highly suppressed in the standard model (SM), as is the direct  $CP$  asymmetry, due to the combination of CKM and GIM suppression:

$$A_{CP} = \frac{\Gamma_{\bar{B}/B^- \rightarrow X_s \gamma} - \Gamma_{B/B^+ \rightarrow X_s \gamma}}{\Gamma_{\bar{B}/B^- \rightarrow X_s \gamma} + \Gamma_{B/B^+ \rightarrow X_s \gamma}} \quad (1.1)$$

The current world average  $A_{CP}$  is  $-(0.8 \pm 2.9\%)$  [1]. The SM prediction for the asymmetry with resolved photon contribution was found in a recent study to be long-distance-dominated and to be in the range  $-0.6\% < A_{CP}^{SM} < 2.8\%$ . Benzke et al. [2] predict a difference in direct  $CP$  asymmetry for charged and neutral  $B$  mesons  $\Delta A_{X_s \gamma} = A_{B^\pm \rightarrow X_s \gamma} - A_{B^0/\bar{B}^0 \rightarrow X_s \gamma}$ . The magnitude of  $\Delta A_{X_s \gamma}$  is proportional to  $\text{Im} \frac{C_{8g}}{C_{7\gamma}}$ , where  $C_{7\gamma}$  and  $C_{8g}$  are Wilson coefficients corresponding to the electro-magnetic dipole transitions and the chromo-magnetic dipole transitions, respectively. The two coefficients are real in the SM and so  $\Delta A_{X_s \gamma}^{SM} = 0$ . New physics contributions could enhance  $\Delta A_{X_s \gamma}$  to be as large as 10%.

The *BABAR* data sample consists of 471 million  $B\bar{B}$  pairs collected at the  $\Upsilon(4S)$  resonance,  $\sqrt{s} = 10.58 \text{ GeV}/c^2$  with the *BABAR* detector at the PEP-II asymmetric-energy  $B$  factory at the SLAC National Accelerator Laboratory. The *BABAR* detector is described in detail in Ref. [3].

$B$  meson candidates from 38 final states with a combination of  $K_s^0$ ,  $K^\pm$ ,  $\pi$ ,  $\eta$  and a photon are reconstructed. Only sixteen modes (ten charged, six neutral) are used for the  $CP$  measurement as the other modes are polluted by the cross feed from a number of other  $B \rightarrow X_s \gamma$  final states with uncertain  $CP$  values. These modes are reconstructed too, so as to veto them after selecting the best candidate. Charged kaons and pions are selected from charged tracks classified with an error-correcting output code algorithm. Neutral kaons are reconstructed from the decay  $K_s^0 \rightarrow \pi^+ \pi^-$ . The invariant mass of the two oppositely charged tracks is required to be between 489 and 507 MeV with a flight distance greater than 0.2 cm from the interaction point. The flight significance (defined as the flight distance divided by the uncertainty of the flight distance) of the  $K_s^0$  must be greater than three. The neutral meson  $\pi^0$  and  $\eta$  are reconstructed from two photons. Each photon is required to have an energy of at least 30 (50) MeV for reconstructing  $\pi^0$  ( $\eta$ ). The invariant mass of the two photons must be in the range of [115,150] ([470,620]) MeV for  $\pi^0$  ( $\eta$ ) candidates. Only  $\pi^0$ s and  $\eta$ s with momentum greater than 200 MeV are used.

Each event is required to have at least one photon with energy  $1.6 < E_\gamma^* < 3.0 \text{ GeV}$ , where the asterisk denotes variables measured in the center of mass (CM) frame. These photons are used as the primary photon in reconstructing  $B$  mesons. This photon must have a lateral moment less than 0.8 and the next nearest calorimeter cluster must be at least 15 cm away. The angle of the photon momentum with respect to the beam axis must satisfy  $-0.74 < \cos \theta < 0.93$ .

The  $X_s$  system includes all daughters of the  $B$  excluding the primary photon and its invariant mass must satisfy  $0.6 < m_{X_s} < 3.2 \text{ GeV}/c^2$ . The  $X_s$  candidate is combined with the primary photon to form a  $B$  candidate, which is required to have an energy-substituted mass  $m_{ES} = \sqrt{s/2 - p_B^{*2}}$  where  $p_B$  is momentum of  $B$  in the CM frame, greater than  $5.24 \text{ GeV}/c^2$ . The difference between half of the beam total energy and the energy of the reconstructed  $B$  in the CM frame,  $|\Delta E| = |E_{beam}^*/2 - E_B^*|$  is required to be  $< 0.15 \text{ GeV}$ . The angle between the thrust axis of the rest of the event and the primary photon must satisfy  $|\cos \theta_{T\gamma}^*| < 0.85$ .

Two random forest classifiers are used [4]. The first identifies the best  $B$  candidate in events with multiple candidates and gives a factor of approximately two better efficiency given the same fake rate compared to the previous *BABAR* analysis [5], which just used  $\Delta E$  minimization; the second separates signal from the continuum background.

To extract the asymmetry, a simultaneous binned likelihood fit is performed to both  $b$  flavors and the result corrected for asymmetries due to the detector response and asymmetries in the backgrounds. We find  $A_{CP} = (1.7 \pm 1.9 \pm 1.0)\%$  where the uncertainties are statistical and systematic, respectively. This is a reduction in statistical uncertainty by  $\sim 1/3$ , due to the improvement on peaking background rejection. Using the extracted value of  $A_{CP}$  for charged and neutral  $B$ ,  $\Delta A_{X,\gamma} = (5.0 \pm 3.9 \pm 1.5)\%$ . Fig. 1 shows the confidence limits (CL) placed on  $\text{Im} \frac{C_{8g}}{C_{7\gamma}}$  from the measured  $\Delta A_{X,\gamma}$  for all possible values of interference amplitude  $\bar{\Lambda}_{78}$  between 17 and 190 MeV.

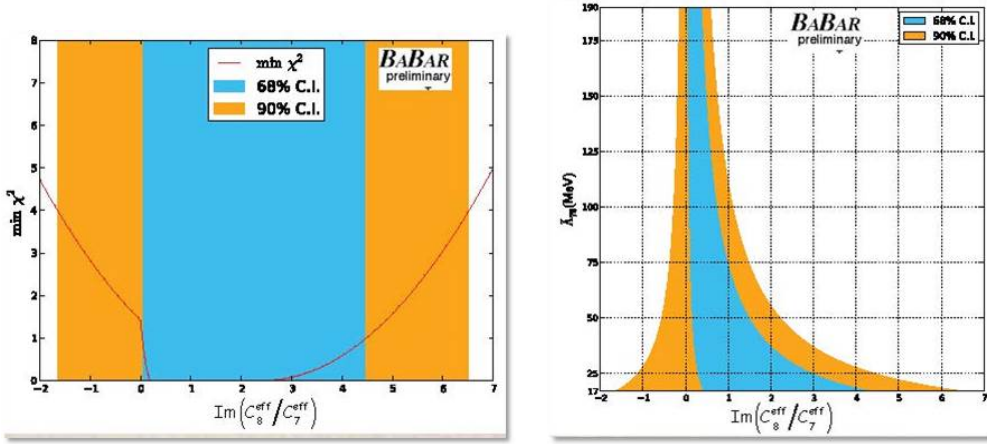


**Figure 1:** Left: Minimum  $\chi^2$  for a given  $\text{Im} \frac{C_{8g}}{C_{7\gamma}}$  from all possible values of  $\bar{\Lambda}_{78}$ . Right: 68% and 90% confidence limits for  $\text{Im} \frac{C_{8g}}{C_{7\gamma}}$  and  $\bar{\Lambda}_{78}$ .

## 2. Search for $B \rightarrow \pi/\eta \ell^+ \ell^-$ [6]

In the SM, the decays  $B \rightarrow \pi \ell^+ \ell^-$  ( $\pi = \pi^\pm, \pi^0$  and  $\ell = e, \mu$ ) and  $B^0 \rightarrow \eta \ell^+ \ell^-$  proceed through the quark-level flavor-changing neutral current (FCNC) process  $b \rightarrow d \ell^+ \ell^-$ . Since all FCNC processes are forbidden at tree level in the SM, the lowest order diagrams representing these transitions must involve loops. For  $b \rightarrow d \ell^+ \ell^-$ , these are the electroweak semileptonic penguin diagrams and the  $W^+ W^-$  box diagrams. The  $b \rightarrow d \ell^+ \ell^-$  transition rate is suppressed by the ratio  $|V_{td}/V_{ts}|^2 \approx 0.04$  compared to  $b \rightarrow s \ell^+ \ell^-$ . The predicted branching fractions for the  $B^+ \rightarrow \pi^+ \ell^+ \ell^-$  and  $B^0 \rightarrow \eta \ell^+ \ell^-$  decay modes are in the range of  $(1.4 - 3.3) \times 10^{-8}$  and  $(2.5 - 3.7) \times 10^{-8}$ , respectively, where the uncertainty is dominated by the lack of knowledge of the  $B \rightarrow \pi$  and  $B^0 \rightarrow \eta$  form factors. Only one  $b \rightarrow d \ell^+ \ell^-$  decay has been observed to date, with LHCb measuring the  $B^+ \rightarrow \pi^+ \mu^+ \mu^-$  branching fraction to be  $(2.3 \pm 0.6 \pm 0.1) \times 10^{-8}$  [7]. Many extensions of the SM predict the existence of new, heavy particles which couple to the SM fermions and bosons.

The *BABAR* data sample corresponds to 471 million  $B\bar{B}$  decays. Two leptons are selected as charged tracks with momenta in the laboratory reference (Lab) frame greater than  $300\text{MeV}/c$ . Loose particle identification (PID) requirements are placed upon the two leptons. The lepton pair is fit to a common vertex to form a dilepton candidate with the requirement that  $m_{\ell\ell} < 5.0\text{GeV}/c^2$ . The energy of the electrons is corrected for Bremsstrahlung emission and photon conversions are suppressed.

Pion PID requirements retain approximately 90-95% of charged pions and only 2-5% of charged kaons. The  $\pi^0$  candidates are reconstructed from two photons with invariant diphoton mass  $m_{\gamma\gamma}$  lying in the range  $115 < m_{\gamma\gamma} < 150\text{MeV}/c^2$ . A minimum value of  $50\text{MeV}$  is required for the Lab energy of each photon. The  $\eta$  meson is reconstructed as  $\eta \rightarrow \gamma\gamma$  ( $\eta_{\gamma\gamma}$ ) and  $\eta \rightarrow \pi^+\pi^-\pi^0$  ( $\eta_{3\pi}$ ). The  $\eta_{\gamma\gamma}$  photon daughters must have energy greater than  $50\text{MeV}$  in the Lab frame. The photon energy asymmetry  $A_\gamma = |E_{1,\gamma} - E_{2,\gamma}|/(E_{1,\gamma} + E_{2,\gamma})$  must be less than 0.8, where  $E_{1,\gamma}$  and  $E_{2,\gamma}$  are the energies of the photons in the Lab frame. The invariant diphoton mass must lie in the range  $500 < m_{\gamma\gamma} < 575\text{MeV}/c^2$ . For  $\eta_{3\pi}$ , the pion candidates are fit to a common vertex to form an  $\eta$  candidate. The  $\eta$  candidate mass is constrained to the nominal  $\eta$  mass, while the invariant three-pion mass is required to lie in the range  $535 < m_{3\pi} < 565\text{MeV}/c^2$ .

The largest source of background comes from random combinations of particles from continuum events or semileptonic  $B$  and  $D$  decays in  $B\bar{B}$  events. Continuum events tend to be jet-like as the  $q\bar{q}$  pair is produced back-to-back with relatively large momentum in the CM frame. The topology of  $B\bar{B}$  decays is more isotropic as the  $B$  mesons are produced nearly at rest in the  $Y(4S)$  rest frame. Semileptonic decays are characterized by the presence of a neutrino, leading to missing energy in the event and non-zero total transverse momentum of the event. Due to the differences in these two background types, four separate artificial neural networks (NNs) are trained to reject  $B\bar{B}$  background in the  $e^+e^-$  modes,  $B\bar{B}$  background in the  $\mu^+\mu^-$  modes, continuum background in the  $e^+e^-$  modes, and continuum background in the  $\mu^+\mu^-$  modes.

To choose the best candidate in event with multiple candidates, a ratio  $\mathcal{L}_R$  from the  $B\bar{B}$  and continuum NN classifier output distributions of the signal and background samples is constructed and the candidate with the greatest value of  $\mathcal{L}_R$  is chosen. The  $\pi\ell^+\ell^-$  and  $\eta\ell^+\ell^-$  branching fractions are extracted through an unbinned extended maximum likelihood fit to  $m_{ES}$  and  $\Delta E$  with the fit region defined as  $m_{ES} > 5.225\text{GeV}/c^2$  and  $-0.3 < \Delta E < 0.25\text{GeV}$ . In addition, lepton-flavor averaged, isospin averaged, and lepton-flavor and isospin averaged results are measured. The twelve upper limits (UL) are shown in Table 2.

### 3. Search for Lepton Number Violation in $B^+ \rightarrow X^-\ell^+\ell'^+$ decays

In the SM, lepton-number and lepton-flavor are conserved but can be violated in high-energy or high-density interactions. The observation of neutrino oscillations indicates that neutrinos have mass and, if the neutrinos are of the Majorana type, the neutrino and antineutrino are the same particle and processes that involve lepton-number violation become possible. Many models beyond the SM predict that lepton-number is violated, possibly at rates approaching those accessible with current data [8]. Lepton-number violation is also a necessary condition for leptogenesis as an explanation of the baryon asymmetry of the Universe.

**Table 1:**  $B \rightarrow \pi \ell^+ \ell^-$  and  $B^0 \rightarrow \eta \ell^+ \ell^-$  branching fractions and branching fraction upper limits (UL) at the 90% CL. The first error quoted on the branching fractions is statistical while the second is systematic.

Mode	$\mathcal{B} (10^{-8})$	UL ( $10^{-8}$ )	Mode	$\mathcal{B} (10^{-8})$	UL ( $10^{-8}$ )
$B^+ \rightarrow \pi^+ e^+ e^-$	$4.3^{+5.9}_{-4.3} \pm 2.0$	12.5	$B^0 \rightarrow \pi^0 e^+ e^-$	$1.3^{+5.4}_{-4.1} \pm 0.2$	8.4
$B^0 \rightarrow \eta e^+ e^-$	$-4.0^{+10.0}_{-8.0} \pm 0.6$	10.8	$B^+ \rightarrow \pi^+ \mu^+ \mu^-$	$-0.7^{+4.4}_{-3.2} \pm 0.9$	5.5
$B^0 \rightarrow \pi^0 \mu^+ \mu^-$	$-0.3^{+5.3}_{-3.6} \pm 0.6$	6.9	$B^0 \rightarrow \eta \mu^+ \mu^-$	$-2.0^{+10.0}_{-6.6} \pm 0.4$	11.2
$B \rightarrow \pi e^+ e^-$	$4.0^{+5.1}_{-4.3} \pm 1.6$	11.0	$B \rightarrow \pi \mu^+ \mu^-$	$-0.7^{+4.1}_{-3.1} \pm 1.2$	5.0
$B^+ \rightarrow \pi^+ \ell^+ \ell^-$	$1.6^{+3.6}_{-3.0} \pm 1.2$	6.6	$B^0 \rightarrow \pi^0 \ell^+ \ell^-$	$0.5^{+3.7}_{-2.9} \pm 0.3$	5.3
$B^0 \rightarrow \eta \ell^+ \ell^-$	$-2.8^{+6.6}_{-5.2} \pm 0.3$	6.4	$B \rightarrow \pi \ell^+ \ell^-$	$1.6^{+3.2}_{-2.7} \pm 1.0$	5.9

A data sample of 471 million  $B\bar{B}$  pairs is used to search for  $B^+ \rightarrow X^- \ell^+ \ell'^+$  with  $X^- = K^-, \pi^-, \rho^-, K^{*-}$  or  $D^-$  and  $\ell^+/\ell'^+ = e^+$  or  $\mu^+$ . Particle identification is applied to all charged tracks. Events are selected that have four or more charged tracks, at least two of which must be identified as leptons. The ratio of the second-to-zeroth Fox-Wolfram moments of the event must be less than 0.5 and the two charged leptons must have the same sign and a momentum greater than 0.3 GeV/ $c$  in the laboratory frame. The separation along the  $z$ -axis between the two leptons at their closest approach to the beamline is required to be less than 0.2 cm. The combined momentum of the  $\ell^+ \ell'^+$  pair in the CM system must be less than 2.5 GeV/ $c$ . Electrons and positrons from photon conversions are removed, where photon conversion is indicated by electron-positron pairs with an invariant mass less than 0.03 GeV/ $c^2$  and a production vertex more than 2 cm from the beam axis.

The  $K^{*-}$  is reconstructed through its decay to  $K_S^0 \pi^-$  and  $K^- \pi^0$ ; the  $\rho^-$  and  $D^-$  are reconstructed through their decays to  $\pi^- \pi^0$  and  $K^+ \pi^- \pi^-$ , respectively. The photons from the  $\pi^0$  must have an energy greater than 0.03 GeV, and the  $\pi^0$  is required to have an energy greater than 0.2 GeV, both measured in the laboratory frame. The reconstructed  $\pi^0$  invariant mass must be between 0.12 and 0.16 GeV/ $c^2$ . The invariant mass of the  $\rho^-$  is required to be between 0.470 and 1.07 GeV/ $c^2$ . The  $K_S^0$  must have an opening angle  $\theta$  between its flight direction (defined as the vector between the  $B$  meson and  $K_S^0$  vertices) and its momentum vector such that  $\cos(\theta) > 0.999$ , a transverse flight distance greater than 0.2 cm, a lifetime significance  $\tau/\sigma_\tau > 10$ , and a reconstructed invariant mass between 0.488 and 0.508 GeV/ $c^2$ . The  $D^-$  invariant mass must be between 1.835 and 1.895 GeV/ $c^2$ . The invariant mass ranges are chosen to allow the background event distributions to be modeled.

The two leptons are combined with either a resonance candidate or a charged track to form a  $B$  meson candidate. The  $B$  candidate is required to be in the kinematic region  $5.240 < m_{ES} < 5.289$  GeV/ $c^2$ ; the  $\Delta E$  range depends on the mode but is always  $|\Delta E| < 0.3$  GeV.

The main backgrounds arise from  $q\bar{q}$ ,  $c\bar{c}$ , and  $B\bar{B}$  events formed from random combinations of leptons from semileptonic  $B$  and  $D$  decays. These are suppressed through the use of a boosted decision tree discriminant (BDT) [9] based on event-shape variables. For the few events with multiple  $B$  candidates remaining, the candidate with the best vertex  $\chi^2$  is chosen.

For each mode, the signal and background yields are extracted from the data with an unbinned maximum likelihood (ML) fit to  $m_{ES}$ ,  $\Delta E$ , and the BDT output; for modes involving a resonance,

the resonance invariant mass is included as a fourth variable. The results of the ML fits to the on-resonance data are summarized in Table 2. A Bayesian approach is taken to calculate the branching fraction UL  $\mathcal{B}_{UL}$  by multiplying the likelihood distributions with a prior which is null in the unphysical regions and constant elsewhere. No significant yields are observed and 90% CL UL are placed on the branching fractions in the range  $(1.5 - 26.4) \times 10^{-7}$ .

**Table 2:** Summary of results for the measured  $B$  decay modes: total number of events in analysis region, signal yield  $n_s$  (corrected for fit bias) and its statistical uncertainty, reconstruction efficiency  $\eta$ , daughter branching fraction product  $\Pi\mathcal{B}_i(\%)$ , significance  $S$  (systematic uncertainties included), measured branching fraction  $\mathcal{B}$ , and the 90% C.L. upper limit ( $\mathcal{B}_{UL}$ ).

Mode	Events	Yield	$\eta(\%)$	$\Pi\mathcal{B}_i(\%)$	$S(\sigma)$	$\mathcal{B}(\times 10^{-7})$	$\mathcal{B}_{UL}(\times 10^{-7})$
$B^+ \rightarrow K^{*-} e^+ e^+$					1.2	$1.7 \pm 1.4 \pm 0.1$	4.0
$K^{*-} \rightarrow K^- \pi^0$	63	$3.8 \pm 3.3$	$11.5 \pm 0.1$	33.3	1.2	$2.1 \pm 1.8 \pm 0.2$	5.1
$K^{*-} \rightarrow K_s^0 \pi^-$	91	$0.8 \pm 3.9$	$12.3 \pm 0.1$	22.8	0.3	$0.6 \pm 2.9 \pm 0.2$	6.0
$B^+ \rightarrow K^{*-} e^+ \mu^+$					0.0	$-4.5 \pm 2.6 \pm 0.4$	3.0
$K^{*-} \rightarrow K^- \pi^0$	117	$-1.9 \pm 4.7$	$7.9 \pm 0.1$	33.3	0.0	$-1.5 \pm 3.8 \pm 0.4$	6.5
$K^{*-} \rightarrow K_s^0 \pi^-$	172	$-5.1 \pm 2.6$	$8.5 \pm 0.1$	22.8	0.0	$-6.0 \pm 2.8 \pm 0.7$	4.2
$B^+ \rightarrow K^{*-} \mu^+ \mu^+$					1.3	$2.4 \pm 1.8 \pm 0.4$	5.9
$K^{*-} \rightarrow K^- \pi^0$	85	$2.3 \pm 1.8$	$6.1 \pm 0.1$	33.3	1.3	$2.0 \pm 1.8 \pm 0.2$	7.0
$K^{*-} \rightarrow K_s^0 \pi^-$	98	$2.0 \pm 1.8$	$5.8 \pm 0.1$	22.8	1.0	$3.1 \pm 2.9 \pm 0.9$	9.8
$B^+ \rightarrow \rho^- e^+ e^+$	411	$-2.1 \pm 5.7$	$12.1 \pm 0.1$	100.0	0.0	$-0.4 \pm 1.0 \pm 0.1$	1.7
$B^+ \rightarrow \rho^- e^+ \mu^+$	1651	$4.6 \pm 11.4$	$10.3 \pm 0.1$	100.0	0.4	$1.0 \pm 2.4 \pm 0.2$	4.7
$B^+ \rightarrow \rho^- \mu^+ \mu^+$	936	$2.9 \pm 6.8$	$7.3 \pm 0.1$	100.0	0.5	$0.9 \pm 2.0 \pm 0.3$	4.2
$B^+ \rightarrow D^- e^+ e^+$	401	$3.9 \pm 4.8$	$10.2 \pm 0.1$	9.13	1.0	$8.8 \pm 8.6 \pm 1.5$	26.4
$B^+ \rightarrow D^- e^+ \mu^+$	549	$1.1 \pm 3.2$	$7.7 \pm 0.1$	9.13	0.5	$3.4 \pm 9.4 \pm 1.1$	21.5
$B^+ \rightarrow D^- \mu^+ \mu^+$	229	$-1.7 \pm 2.5$	$5.7 \pm 0.1$	9.13	0.0	$-6.5 \pm 9.9 \pm 0.9$	17.4
$B^+ \rightarrow K^- e^+ \mu^+$	117	$5.5 \pm 3.5$	$15.2 \pm 0.1$	100.0	1.8	$0.6 \pm 0.5 \pm 0.1$	1.6
$B^+ \rightarrow \pi^- e^+ \mu^+$	464	$3.8 \pm 3.5$	$16.4 \pm 0.2$	100.0	1.2	$0.5 \pm 0.5 \pm 0.1$	1.5

## References

- [1] Heavy Flavor Averaging Group (HFAG), [www.slac.stanford.edu/xorg/hfag.org](http://www.slac.stanford.edu/xorg/hfag.org).
- [2] M. Benzke, S. J. Lee, M. Neubert and G. Paz, Phys. Rev. Lett. **106**, 141801 (2011).
- [3] B. Aubert *et al.* (BABAR Collaboration), Nucl. Instrum. Methods Phys. Res., Sect. A **729**, 615 (2013).
- [4] L. Breiman, Machine Learning, **45**, 5 (2001).
- [5] B. Aubert *et al.* (BABAR Collaboration), Phys. Rev. Lett. **101**, 171804 (2008).
- [6] J. P. Lees *et al.* (BABAR Collaboration), Phys. Rev. D **88**, 032012 (2013).
- [7] R. Aaij *et al.* (LHCb Collaboration), J. High Energy Phys. **12** 125 (2012).
- [8] A. Atre, T. Han, S. Pascali, and B. Zhang, JHEP 0905:030 (2009).
- [9] B. P. Roe, H.-J. Yang, J. Zhu, I. Stancu, and G. McGregor, Nucl. Instrum. Methods Phys. Res., Sect. A **543**, 577 (2005).